Best Protocol for Combined Contrast-Enhanced Thoracic and Abdominal CT for Lung Cancer: A Single-Institution Randomized Crossover Clinical Trial

Elena García-Garrigós[1]
Juan José Arenas-Jiménez[1]
José Sánchez-Payá[2]

OBJECTIVE. The purpose of this study was to evaluate the superiority of either of two protocols for combined contrast-enhanced thoracic and abdominal CT of patients with lung cancer by comparing contrast enhancement, contrast-related artifacts, image quality, and radiation dose.

SUBJECTS AND METHODS. In this randomized controlled crossover clinical trial, 77 patients who underwent 203 CT examinations were enrolled. All patients underwent at least two examinations performed with both protocols. Protocol A consisted of two acquisitions: one 35-second delayed CT acquisition for the chest followed by a 70-second delayed abdominal acquisition. Protocol B was a single 60-second delayed acquisition covering the chest and the abdomen. Attenuation and noise of the aorta, pulmonary artery, and liver were measured. Contrast-related artifacts, mediastinal lymph node visualization, liver enhancement, and noise were visually scored. Dose-length product was recorded. Statistical analysis was performed by *t* and chi-square tests and kappa statistics.

RESULTS. Contrast-related artifacts were more severe at all evaluated levels, and visualization of lymph node regions was statistically significantly worse with protocol A. There were no differences in enhancement or noise score of the liver. Tumor delineation and pleural findings were better evaluated with delayed phase images. Dose-length product was significantly higher with protocol A (645.0 vs 521.5 mGy · cm; $p < 0.0001$).

CONCLUSION. A single 60-second delayed acquisition for thoracic and abdominal contrast-enhanced CT is associated with less contrast artifact and affords better visualization of lymph nodes at a lower radiation dose while acceptable vascular and hepatic contrast enhancement is maintained.

Keywords: contrast injection protocol, CT, lung cancer, pleural malignancy, radiation dose

doi.org/10.2214/AJR.17.19185

Received October 18, 2017; accepted after revision November 23, 2017.

Based on a presentation at the 2017 World Congress of Thoracic Imaging, Boston, MA.

Supported by Fundación para el Fomento de la Investigación Sanitaria y Biomédica de la Comunitat Valenciana (ISABIAL)-FISABIO (grant no. UGP-16-141).

[1]Department of Radiology, Hospital General Universitario de Alicante, Instituto de Investigación Sanitaria y Biómedica de Alicante (ISABIAL), FISABIO Hospital General Universitario de Alicante, Av Pintor Baeza 12, 03010, Alicante, Spain. Address correspondence to J. J. Arenas-Jiménez (arenas_jua@gva.es).

[2]Department of Epidemiology, Hospital General Universitario de Alicante, Instituto de Investigación Sanitaria y Biómedica de Alicante (ISABIAL), FISABIO Hospital General Universitario de Alicante, Alicante, Spain.

Supplemental Data
Available online at www.ajronline.org.

AJR 2018; 210:1226–1234

0361–803X/18/2106–1226

Contrast-enhanced CT of the chest and upper abdomen has an important role in the initial workup and follow-up of lung cancer and is one of the examinations most frequently requested of thoracic radiologists. Standard guidelines in the management of lung cancer [1–5] include both chest and upper abdominal contrast-enhanced CT.

The introduction of MDCT technology has dramatically decreased scanning time, making it necessary to adjust contrast injection and scanning parameters to the capabilities of these new technologies [6]. The role of iodinated contrast medium in these examinations is to achieve adequate depiction of hilar and mediastinal vascular structures together with optimal enhancement of tumoral lesions and abdominal viscera. The literature on scanning parameters for routine chest or combined chest and abdominal CT is limited; a few reports have focused on the influence of contrast concentration [7–11] and kilovoltage [12–14]. Protocols vary among institutions according to the technical characteristics of equipment and personal preferences of radiologists.

Many parameters affecting the quality of examinations and their accuracy must be taken into account when designing a contrast-enhanced CT protocol. These include CT acquisition parameters (length, kilovoltage, milliamperage), patient characteristics (weight, height, cardiovascular condition), and the contrast medium (quantity, concentration, rate of injection, delay) [6]. No single standardized protocol exists for performing combined thoracic and abdominal CT, and imaging guidelines for lung cancer lack specific scanning protocol recommendations [1–5]. When a protocol is suggested, the level of evidence is low and primarily based on expert opinion [15–18].

In contemporary clinical practice with newer technologies, there are two commonly

accepted methods for performing combined contrast-enhanced CT of the chest and abdomen. The first incorporates a single delayed acquisition that includes the chest and upper abdomen. The second method consists of two independent CT acquisitions: CT of the chest in an early phase after contrast injection and CT of the upper abdomen including the liver in a portal phase. Protocol recommendations [15–18] and literature including data about scanning protocols [7–14, 19, 20] also are divided on the use of one or two separate acquisitions for combined chest and abdominal CT. It is therefore unclear whether a single delayed phase acquisition of the chest and abdomen provides adequate vascular attenuation of the chest while maintaining adequate image quality in the abdomen.

The purpose of our study was to evaluate the superiority of either of two protocols (single vs dual acquisition) for combined contrast-enhanced thoracic and abdominal CT in patients with lung cancer by comparing contrast enhancement, contrast-related artifacts, image quality, and radiation dose. The double acquisition protocol included two independent acquisitions of the chest (early phase) and the abdomen (delayed phase). The single scan acquisition included both the chest and abdomen in the delayed phase.

Subjects and Methods

This prospective randomized controlled crossover clinical trial was reviewed and approved by the institutional review board and local ethics committee. Written informed consent was obtained from all participants in the study.

Patient Population

From May to December 2015, patients referred to our department for combined chest and abdominal contrast-enhanced CT as initial workup or follow-up of lung cancer were enrolled in the study. Patients were excluded if they had an estimated glomerular filtration rate less than 60 mL/min, if they had an allergy to iodinated contrast material, or if the contrast injection protocol could not be achieved as required owing to inadequate vein access, extravasation, or any other problem during contrast injection. Patients weighing less than 50 kg or more than 100 kg were excluded. When the patients were enrolled, they were initially randomized to one of the two scanning protocols, A or B. On each subsequent imaging visit, the other protocol was used.

We initially enrolled 419 patients in the study for a total of 557 CT examinations. The patient enrollment flowchart is shown in Figure 1. After

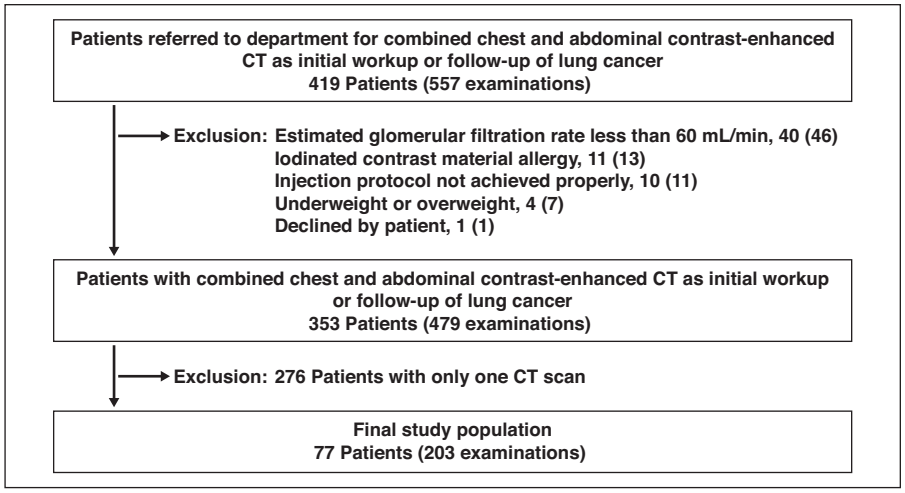

Fig. 1—Flowchart shows exclusion and inclusion criteria for study. Values in parentheses are number of CT examinations.

TABLE 1: Patient Demographic Data and Tumor Characteristics

Characteristic	Value
Sex	
Male	55 (71.4)
Female	22 (28.6)
Age (y)	64.1 (42–83)
Weight (kg)	71.6 (50–100)
Height (cm)	166.3 (150–182)
Histologic result	
Adenocarcinoma	40 (51.9)
Squamous	20 (26.0)
Small cell	15 (19.5)
Non–small cell (not otherwise specified)	2 (2.6)
Stage	
IA	6 (7.8)
IB	5 (6.5)
IIA	4 (5.2)
IIB	2 (2.6)
IIIA	7 (9.1)
IIIB	4 (5.2)
IV	49 (63.6)
Treatment	
Chemotherapy	43 (55.8)
Chemoradiotherapy	17 (22.1)
Surgery	13 (16.9)
Surgery and chemotherapy	3 (3.9)
Radiotherapy	1 (1.3)

Note—Values are number of patients with percentage in parentheses or mean with range in parentheses. Stage is based on the system set out in the 7th edition of the American Joint Committee on Cancer lung cancer staging manual.

exclusions, the final study population consisted of 203 scans of 77 patients. Patient characteristics, histologic results, staging, and treatments are detailed in Table 1. The number of CT examinations per patient ranged from two to six; 101 were performed with protocol A and 102 with protocol B. Weight and height were obtained from patient clinical charts. There were no statistically significant differences in patient sex, age, weight, or height in the two protocol groups.

CT Protocols

All CT scans were obtained with a 16-MDCT scanner (Somatom Emotion 16, Siemens Healthcare). Protocol A consisted of two acquisitions, one of the chest ending at the lung bases beginning 35 seconds after the initiation of contrast administration. This was followed by a 70-second delayed abdominal acquisition starting at the dome of the diaphragm and extending inferiorly. In this way there was always overlap of the two acquisitions. In protocol B, the acquisition coverage was the same as in protocol A, but a single acquisition was performed at 60-second delay.

In both protocols scanning was performed in the craniocaudal orientation with the patient in supine position with arms above the head. Acquisition began approximately 2 cm above the lung apices to include the supraclavicular regions and extended through the upper abdomen to include the whole liver.

Scan parameters for protocol A were as follows: collimation, 16 × 1.5 mm; pitch, 1.2; rotation time, 0.6 second; reference tube current–time products, 150 mAs for the chest and 200 mAs for the abdomen at 110 kVp. Scan parameters for protocol B were as follows: collimation, 16 × 1.5 mm; pitch, 1.2; rotation time, 0.6 second; reference tube current–time product, 170 mAs at 110 kVp. Automatic tube current modulation (CARE Dose 4D, Siemens Healthcare) was switched on for all examinations.

Image reconstruction was performed with a medium-smooth soft-tissue kernel (B30) at a slice thickness of 5 mm without overlap and a slice thickness of 2 mm with 1.2-mm interval (one independent series each for the chest and another for the abdomen) and with a high-spatial-frequency reconstruction kernel (B70) at a slice thickness of 2 mm with 1.2-mm interval for the chest. Finally, five series were reconstructed for each patient and sent to the PACS in the same order for all patients independently of the scanning protocol used. All images were reviewed at a PACS workstation at window settings appropriate for viewing the lung parenchyma (level, –700 HU; width, 1500 HU) and the mediastinum (level, 50 HU; width, 400 HU).

All patients received a standardized IV injection through a power injector consisting of iomeprol (Iomeron, Bracco) with either 350 or 400 mg I/mL at a dose of 0.5 g I/kg body weight fixed 40-second duration of injection followed by a 30-mL saline chaser at the same rate as for the contrast medium. Contrast concentration was not controlled and was subject to availability at the time of the CT examination. No specific instructions were given to the technicians to choose a specific concentration. Dose-length product provided by the CT scanner was recorded for each examination.

Image Analysis

Two thoracic radiologists (10 and 20 years of thoracic CT interpretation experience) blinded to the acquisition protocol independently reviewed CT images at a PACS workstation (Centricity PACS Universal Viewer 6.0, GE Healthcare). They were instructed to begin reading at the 5-mm abdominal series to avoid interpretation bias due to knowledge of the imaging protocols, which can be more apparent in chest series.

Quantitative assessment—Quantitative assessment was performed by placing a circular ROI of approximately 1.5 cm^2 in the 5-mm-thickness reconstructions and measuring attenuation values in Hounsfield units. Thoracic vascular attenuation measurements were performed in the pulmonary trunk at the level of the bifurcation and in the ascending and descending thoracic aorta, all at the same slice level. Abdominal attenuation measurements were in the left hepatic lobe, anterior and posterior right hepatic lobes, right erector spinae muscle, spleen, and aorta at the level of the main portal vein, all at the same slice level.

The size of the ROI in the muscle was adapted to avoid inclusion of fat in the measurement. Vessels, bile ducts, focal steatosis, and other focal lesions were avoided when placing the ROI in the liver and spleen. When there was clearly prominent diffuse hepatic steatosis, liver attenuation measurements from that patient were excluded from analysis by consensus of the two readers. SD of the measurement of the anterior right hepatic lobe was registered as image noise. Mean attenuation of the liver was calculated as the average of the three hepatic measurements. Contrast-to-noise ratio (CNR) and signal-to-noise ratio (SNR) of the liver were calculated according to the following formulas [13, 21]: CNR = (mean attenuation of the liver – ROI attenuation of the muscle) / noise of the liver; SNR = mean attenuation of the liver / noise of the liver.

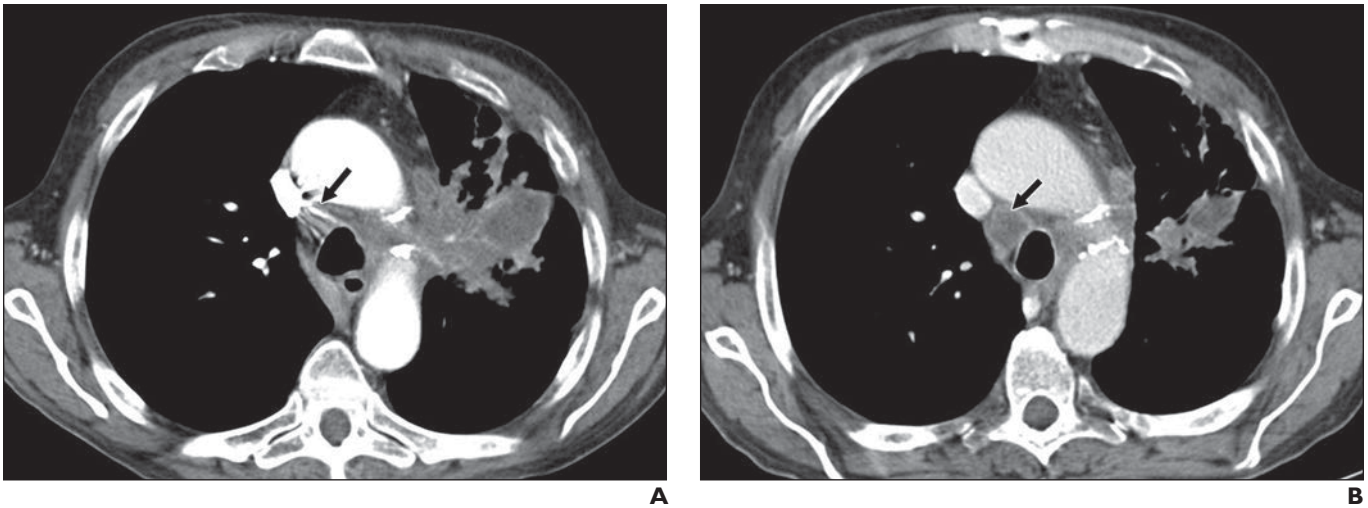

Fig. 2—57-year-old man with squamous lung carcinoma.
A and **B**, Axial contrast-enhanced helical CT scans obtained with protocols A (**A**) and B (**B**) show severe perivenous artifact limiting evaluation of lymph node at 4R nodal station (*arrow*). Protocol B (**B**) shows absence of perivenous artifacts and excellent delimitation of node at 4R station (*arrow*).

TABLE 2: Quantitative Analysis Results for Protocols A and B

Characteristic	Reader	Protocol A (n = 101) Mean	Protocol A (n = 101) SD	Protocol B (n = 102) Mean	Protocol B (n = 102) SD	p
Pulmonary artery attenuation (HU)	1	331.8	75.6	200.6	23.8	0.000
	2	329.5	73.1	199.7	22.9	0.000
Pulmonary artery noise (HU)	1	12.5	2.5	10.1	2.1	0.000
	2	13.4	2.6	10.6	1.9	0.000
Ascending aorta attenuation (HU)	1	317.2	50.8	203.0	28.4	0.000
	2	312.5	57.2	202.3	27.5	0.000
Descending aorta attenuation (HU)	1	297.1	48.7	193.1	32.4	0.000
	2	295.4	51.7	194.9	30.8	0.000
Abdominal aorta attenuation (HU)	1	166.7	22.2	185.5	25.7	0.000
	2	167.2	20.2	183.6	24.2	0.000
Anterior right hepatic lobe attenuation (HU)[a]	1	118.6	14.1	122.2	14.3	0.081
	2	117.5	18.1	120.6	16.7	0.208
Anterior right hepatic lobe noise (HU)	1	12.2	2.6	12.3	3.0	0.752
	2	11.9	2.1	12.4	2.7	0.154
Posterior right hepatic lobe attenuation (HU)[a]	1	113.9	13.4	117.2	13.7	0.090
	2	113.5	13.0	116.2	13.8	0.161
Left hepatic lobe attenuation (HU)[a]	1	120.9	15.5	124.1	14.3	0.129
	2	119.8	14.4	124.8	13.4	0.011
Mean hepatic attenuation (HU)[a]	1	117.8	13.5	121.2	12.4	0.070
	2	116.9	13.8	120.5	13.1	0.059
Splenic attenuation (HU)	1	118.3	12.5	134.5	19.0	0.000
	2	118.6	11.7	134.5	17.2	0.000
Hepatic contrast-to-noise ratio[a]	1	5.7	1.8	6.1	2.1	0.240
	2	5.7	1.6	5.7	1.8	0.892
Hepatic signal-to-noise ratio[a]	1	10.1	2.6	10.5	2.9	0.432
	2	10.1	2.2	10.1	2.5	0.889
Dose-length product (mGy · cm)		645.0	159.9	521.5	96.7	0.000

[a] n = 100 in protocol A and n = 101 in protocol B owing to exclusion of one patient with diffuse hepatic steatosis.

Qualitative analysis—Qualitative analysis was performed in 5-mm-thick reconstructions. Perivenous artifacts at three levels (subclavian and axillary veins on the side of injection, supraclavicular region on the side of injection, and bilateral brachiocephalic veins or superior vena cava) were graded as follows: 1, no artifact; 2, artifact present not interfering with evaluation; 3, severe artifact limiting evaluation. Similarly, evaluation of potential lymph nodes adjacent to the vessels in the axillary and subclavian regions, supraclavicular region, levels 2R and 2L, and level 4R was graded according to the following scale: 1, excellent, vessels and surrounding tissue clearly defined; 2, good, some evident artifacts present but not limiting evaluation; 3, poor, severe artifacts potentially limiting lymph node margins and subsequent measurements.

Presence of possible atelectasis associated with the tumor was evaluated. When it was found, observers were asked to grade tumor delineation from surrounding tissues in the chest series on the following scale: 1, excellent delineation of the tumor; 2, acceptable differentiation of tumor margins from possible atelectasis; and 3, bad delineation of the tumor. They also evaluated the presence of pleural effusion; when they found it, they graded visualization of pleural thickening or nodules according to the following scale: 1, excellent definition; 2, acceptable definition; 3, poor definition. In the same way, they were asked to determine the visual assessment of the liver on the following scale: 1, excellent definition; 2, acceptable definition; 3, poor definition.

The presence of hepatic metastases was evaluated, and if there were any suspicious lesions, qualitative analysis of tumor conspicuity was performed independently in the thoracic and abdominal series with the same criteria as for the liver. Finally, noise in the liver images was subjectively graded on the following 5-point scale: 1, no appreciable noise;

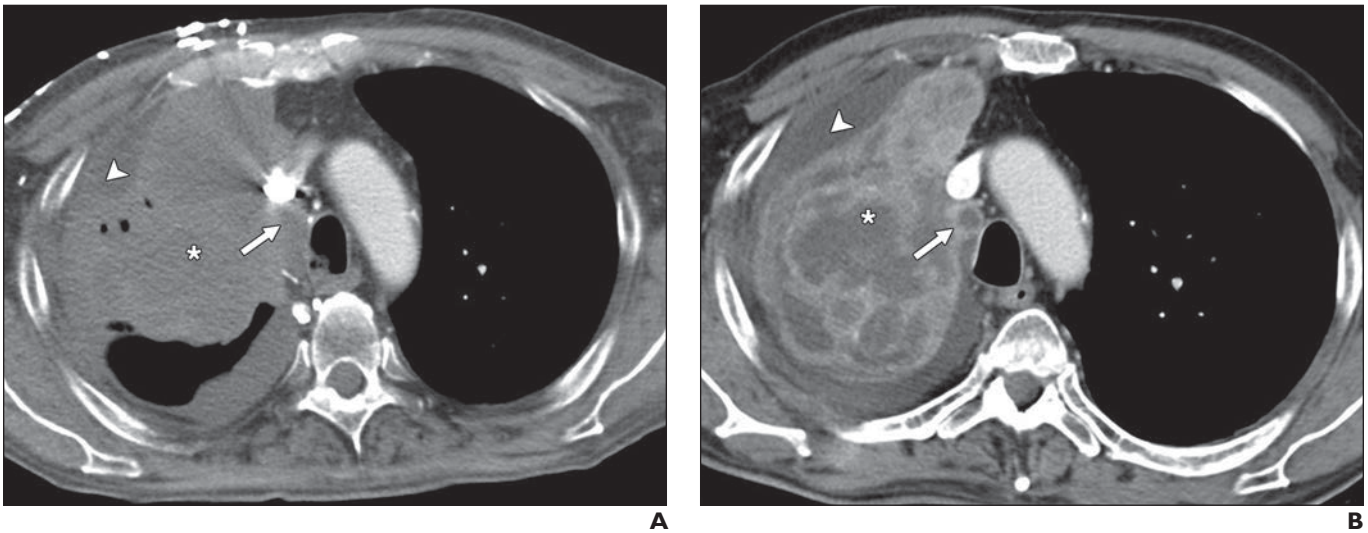

Fig. 3—64-year-old man with lung adenocarcinoma.
A and **B,** Axial contrast-enhanced helical CT scans were obtained with protocols A (**A**) and B (**B**). Protocol A (**A**) shows poor tumor delineation (*asterisk*) from pleural effusion (*arrowhead*) and 4R lymph node (*arrow*). Perivenous artifact is present at superior vena cava. Scan obtained 3 months later using protocol B (**B**) shows excellent differentiation of the tumor (*asterisk*), pleural effusion (*arrowhead*), and 4R lymph node (*arrow*).

2, minimum noise; 3, average noise not disturbing liver evaluation; 4, above average noise; 5, too much noise, potentially limiting evaluation.

Presence or absence of pulmonary embolism was assessed on 2-mm-thickness images. When present it was classified as central (segmental or proximal pulmonary arteries), peripheral, or both.

Statistical Analysis

The two protocol groups were compared by chi-square test for sex and age and unpaired *t* test for weight and height. The quantitative measurements between the two protocol groups and between iodine concentrations were compared by *t* test. A paired *t* test was used to compare consecutive measurements between the two protocols in the same patient. The qualitative analysis results were compared between protocols by chi-square test. Weighted kappa statistics were used to measure the degree of agreement between observers in evaluation of qualitative variables. Statistical analysis was performed with the software package SPSS Statistics (version 21, IBM). Statistical significance was set at 0.05.

Results

Quantitative Assessment

The mean enhancement of the pulmonary artery, ascending aorta, and descending aorta was significantly greater with protocol A than with protocol B for both independent observers (Table 2). Pulmonary artery enhancement was less than 150 HU in two examinations performed with protocol B and less than 211 HU in five performed with protocol A. There were no statistically significant differences in any abdominal liver attenuation measurements or in calculated abdominal CNR and SNR measurements except for left hepatic lobe attenuation by reader 2, which was higher with protocol B (Table 2). There was statistically significant greater enhancement of the spleen and abdominal aorta with protocol B. When paired *t* test analysis was performed on a subset of 182 consecutive examinations (91 paired consecutive examinations with protocol A and B in the same patients), differences between protocols were also statistically significant in the thoracic vessels, spleen, and abdominal aorta for both readers.

Regarding the effect of contrast iodine concentration, pulmonary artery attenuation with protocol A showed greater enhancement with the lower concentration of iodinated contrast medium. There was otherwise no statistically significant difference in vascular or parenchymal enhancement between the two iodine concentration groups (Table S1).

Dose-length product was statistically significant higher with protocol A than with

TABLE 3: Qualitative Analysis Results for Protocols A and B

Grade	Protocol A (*n* = 101)	Protocol B (*n* = 102)	*p*
Axillary lymph nodes			0.000
Reader 1			
1	2 (2.0)	27 (26.5)	
2	1 (1.0)	38 (37.3)	
3	98 (97.0)	37 (36.3)	
Reader 2			0.000
1	1 (1.0)	35 (34.3)	
2	2 (2.0)	35 (34.3)	
3	98 (97.0)	32 (31.4)	
Supraclavicular lymph nodes			
Reader 1			0.000
1	0 (0.0)	58 (56.9)	
2	16 (15.8)	35 (34.3)	
3	85 (84.2)	9 (8.8)	
Reader 2			0.000
1	0 (0.0)	71 (69.6)	
2	19 (18.8)	22 (21.6)	
3	82 (81.2)	9 (8.8)	
2R Lymph nodes			
Reader 1			0.000
1	6 (5.9)	102 (100.0)	
2	37 (36.7)	0 (0.0)	
3	58 (57.4)	0 (0.0)	
Reader 2			
1	6 (5.9)	99 (97.0)	
2	28 (27.7)	2 (2.0)	
3	67 (66.3)	1 (1.0)	
4R Lymph nodes			
Reader 1			0.000
1	5 (5.0)	102 (100.0)	
2	41 (40.6)	0 (0.0)	
3	55 (54.5)	0 (0.0)	
Reader 2			0.000
1	5 (5.0)	102 (100.0)	
2	35 (34.6)	0 (0.0)	
3	61 (60.4)	0 (0.0)	
Hepatic parenchymal enhancement			
Reader 1			0.474
1	97 (96.0)	97 (95.1)	
2	3 (3.0)	5 (4.9)	
3	1 (1.0)	0 (0.0)	
Reader 2			0.745
1	97 (96.0)	97 (95.1)	
2	4 (4.0)	5 (4.9)	
3	0 (0.0)	0 (0.0)	

(Table 3 continues on next page)

TABLE 3: Qualitative Analysis Results for Protocols A and B (continued)

Grade	Protocol A (*n* = 101)	Protocol B (*n* = 102)	*p*
Hepatic noise			
Reader 1			0.204
1	0 (0.0)	0 (0.0)	
2	32 (31.7)	34 (33.3)	
3	69 (68.3)	65 (63.7)	
4	0 (0.0)	3 (2.9)	
5	0 (0.0)	0 (0.0)	
Reader 2			0.697
1	0 (0.0)	0 (0.0)	
2	44 (44.0)	40 (39.2)	
3	56 (55.0)	60 (58.8)	
4	1 (1.0)	2 (2.0)	
5	0 (0.0)	0 (0.0)	
Axillary artifact			
Reader 1			0.000
1	1 (1.0)	17 (16.7)	
2	0 (0.0)	46 (45.1)	
3	100 (99.0)	39 (38.2)	
Reader 2			0.000
1	1 (1.0)	25 (24.5)	
2	2 (2.0)	43 (42.2)	
3	98 (97.0)	34 (33.3)	
Supraclavicular artifact			
Reader 1			0.000
1	2 (2.0)	47 (46.1)	
2	7 (6.9)	47 (46.1)	
3	92 (91.1)	8 (7.8)	
Reader 2			0.000
1	0 (0.0)	66 (64.7)	
2	18 (17.8)	27 (26.5)	
3	83 (82.2)	9 (8.8)	
Caval artifact			
Reader 1			0.000
1	2 (2.0)	98 (96.1)	
2	34 (33.7)	4 (3.9)	
3	65 (64.4)	0 (0.0)	
Reader 2			0.000
1	2 (2.0)	96 (94.1)	
2	32 (31.7)	6 (5.9)	
3	67 (66.3)	0 (0.0)	

Note—Values in parentheses are percentages.

B (645.0 ± 159.9 vs 521.5 ± 96.7 mGy · cm; $p < 0.0001$) because of overlap of thoracic and abdominal acquisitions and a higher reference tube current–time product for the abdomen.

Visual Assessment

Contrast-related perivenous artifacts (Fig. 2) were more severe with protocol A for all levels evaluated, and the difference was statistically significant (Table 3). Subsequently, mediastinal lymph nodes levels were judged to be evaluated worse with protocol A than with B. Neither liver assessment score nor subjective noise grade exhibited statistically significant differences between protocols (Table 3).

TABLE 4: Kappa Correlation Between Readers in Qualitative Variables Assessment

Variable	κ
Axillary lymph nodes	0.760
Supraclavicular lymph nodes	0.800
2R Lymph nodes	0.845
4R Lymph nodes	0.854
Hepatic parenchymal enhancement	0.884
Hepatic noise	0.556
Axillary vein artifact	0.710
Supraclavicular vein artifact	0.715
Vena cava artifact	0.881

Agreement between observers was good to excellent for the qualitative variables, except for hepatic noise evaluation, which had a kappa value of 0.556 (Table 4). Tumor delineation was evaluated by readers 1 and 2 using both protocols for 19 readings in 14 patients. Protocol B performed better than protocol A (Fig. 3) in 13 cases interpreted by reader 1 and 10 cases by reader 2. In contrast, only one reading performed better with protocol A than with protocol B.

The thoracic phase was compared with the abdominal phase of protocol A for grading of pleural findings, including pleural thickening and nodules associated with pleural effusions in 37 examinations. In 18 cases, both observers scored pleural findings better during the abdominal phase of protocol A (Fig. 4). Mean scores for both protocol B and the abdominal phase of protocol A (reader 1, 1.28; reader 2, 1.19) were better than for the early phase of protocol A (reader 1, 1.83; reader 2, 1.72; $p < 0.001$), a score of 1 being excellent definition and 3 poor definition of pleural findings.

Hepatic metastases were evaluated by both observers for 20 examinations of nine patients. There was no interobserver disagreement on lesion detectability between protocols A and B. Nine examinations were performed with protocol A. In three of them, both thoracic and abdominal phases were graded 1 by both observers. In the other six examinations, observers scored the abdominal phase better than the thoracic phase.

Pulmonary embolism was diagnosed in eight patients, five with protocol A (one central, four both central and peripheral) and three with protocol B (one central, one peripheral, and one both central and peripheral). When available, previous CT scans were reviewed for potentially missed pulmonary emboli, although none were discovered.

Discussion

Contrast-enhanced CT of the chest and upper abdomen plays an essential role in staging and follow-up of lung cancer. However, appropriate recommendations for the optimal scanning protocol are lacking. The goals of the radiologist in combined contrast-enhanced CT of the chest and abdomen are to achieve optimal contrast opacification of systemic and pulmonary vessels, avoid contrast-related artifacts, and obtain adequate contrast enhancement of lesions, the liver, and other viscera.

In clinical practice, two distinct protocols exist for combined contrast-enhanced chest and abdominal CT. The first is similar to that used in classic single-detector scanners with one early (20- to 35-second delayed) acquisition for the chest and a second delayed portal venous phase for the abdomen. The second protocol consists of a single acquisition covering the whole chest and upper abdomen with a scanning delay that includes the liver during the portal venous phase. However, information is lacking about the advantages and disadvantages of these protocols, more specifically, whether a single delayed acquisition of the chest and abdomen provides adequate vascular enhancement in the chest while maintaining image quality in the abdomen. In this setting, we conducted a randomized trial to evaluate these protocols and determine whether differences exist between these scanning options.

A primary concern with use of an early phase in contrast-enhanced chest CT, is the presence of perivenous artifacts caused by concentrated contrast medium entering through the superior vena cava. When severe, these artifacts can blur perivascular structures and limit evaluation of mediastinal lymph nodes, particularly the superior mediastinal chains. Use of a saline chaser bolus after contrast injection reduces contrast dose and artifacts in the chest [22, 23], although this has no effect on liver enhancement [24]. In our series, the frequency of substantial contrast-related perivenous artifacts in protocol A was greater than that in other studies [8, 22, 23]. However, most of the patients in those studies received a lower total dose of iodine and had shorter injection times than our patients did. Regarding contrast-related perivenous artifacts, our results show benefits of a 60-second delayed chest scan. The reasons for this are likely twofold. On one hand, the contrast delay with saline push promotes appropriate contrast washout and clearing of the veins [23]. On the other hand, contrast medium is already recirculating, resulting in optimal, homogeneous enhancement of jugular, subclavian, and brachiocephalic veins and the superior vena cava [6, 25].

As expected, there were obvious differences in contrast enhancement of thoracic vessels between the two protocols; greater attenuation was found in the early phase of protocol A than in protocol B for all levels analyzed. In the vast majority of patients, attenuation values for the aorta and pulmonary artery were greater than 200 HU with protocol A, a level acceptable for angiographic studies. For protocol B, levels were greater than 150 HU in most patients, a value considered acceptable for routine chest scanning [17]. More than 93% of patients undergoing protocol A had attenuation greater than 211 HU, a value that Wittram [26] suggested is the theoretic minimum attenuation required to see pulmonary venous thromboemboli; only 35% of patients receiving protocol B did so. From our point of view, however, attenuation values achieved in protocol B are suitable for routine clinical evaluation of the mediastinal and vascular structures with chest CT. It can be assumed that protocol B is less effective for detecting pulmonary emboli, but in general we are not seeking pulmonary emboli when performing CT for lung cancer evaluation. Although unsuspected pulmonary embolism involving peripheral pulmonary arteries is fairly frequent in this population [27], this would not make us change our primary imaging objectives.

One of the advantages of delayed scanning of the chest is theoretic optimal contrast

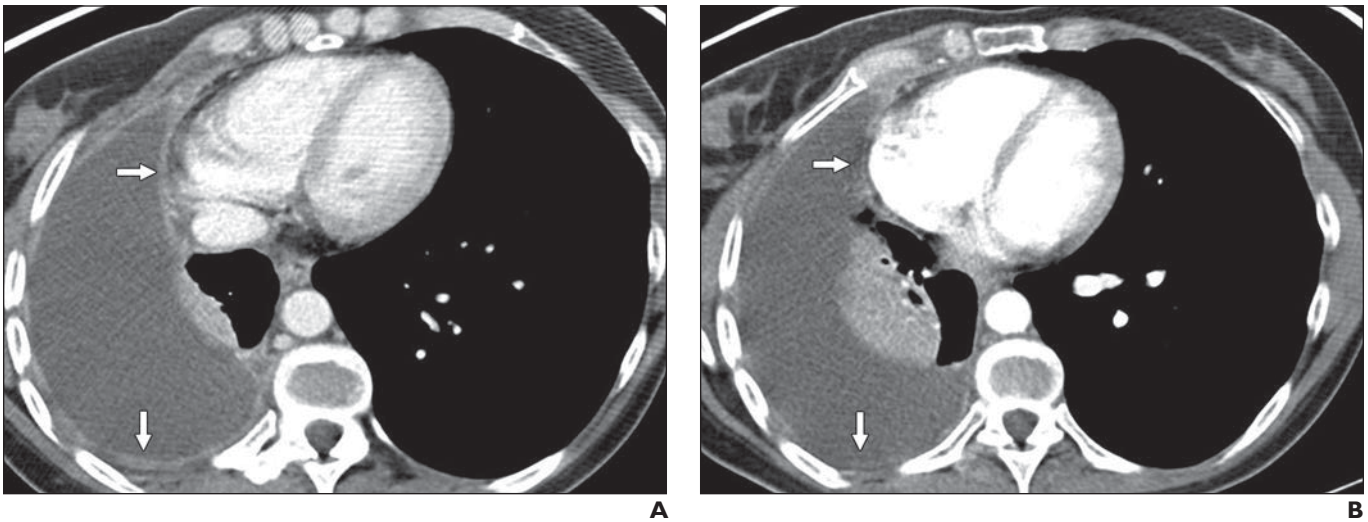

Fig. 4—48-year-old woman with lung adenocarcinoma and metastatic pleural effusion.
A, Axial contrast-enhanced helical CT scan obtained with protocol B shows excellent definition of pleural thickening at costal and mediastinal pleura (*arrows*) graded 1 by both observers.
B, Axial early phase contrast-enhanced CT scan obtained with protocol A 3 months after **A** shows acceptable definition of pleural thickening (*arrows*) graded 2 by both observers.

opacification of tumoral lesions due to timing of the contrast bolus, greater contrast distribution occurring in the extravascular interstitial space. In thoracic imaging, this is particularly relevant for evaluation of pleural thickening, tumoral lesions accompanying pleural effusions, and differentiation and delineation of lung tumors. The British Thoracic Society statement on malignant mesothelioma [16] recommends a 60-second delayed scan for this specific reason. Pleural thickening or nodules can be difficult to distinguish during the early phases of contrast-enhanced chest CT owing to lack of contrast enhancement. This is particularly true in comparisons of data from pulmonary CT angiography with data from routine thoracic CT during the venous phase, as shown in a recent report [28] on the diagnostic performance of routine CT in patients with suspected pleural malignancy. Using 60-second delayed scanning, Raj et al. [29] found greater contrast of pleural surfaces using higher doses of contrast medium. In our series, images from the abdominal phase in either protocol A or protocol B scored better than the early phase of the chest scan. Regarding delineation of lung tumors, their appearance and differentiation from atelectasis is variable. According to our results, however, in 14 patients with persistent tumoral lesions and atelectasis on two consecutive scans, protocol B was superior to protocol A in most cases.

To our knowledge, no study has systematically evaluated the need for an arterial phase of the liver in imaging of metastases of lung cancer. Therefore, these CT scans are usually obtained only in the portal phase [9, 19]. In our series, liver lesion definition was considered better in the delayed abdominal phase than in the thoracic phase in 66% of scans showing metastases in both phases. For adequate tumor–to–normal liver contrast, the most important factors to be considered are the total amount of iodine delivered and body weight [6, 19]. For this reason, protocols for patients with cancer must take into consideration the contrast dose adapted to the patient's specific body characteristics, as in our study. Although other body size indexes have been suggested [30], body weight at doses of 0.5–0.6 g I/kg is the most frequently used owing to its simplicity [17, 19, 31, 32]. Contrast enhancement, noise, calculated CNR and SNR, and visual assessment of the liver were not different for the portal phases of the two protocols, making both abdominal phases equivalent in terms of enhancement and quality. Moreover, attenuation of the spleen and abdominal aorta was even higher with protocol B.

As also shown in other studies [8, 9], use of protocol A resulted in a higher degree of enhancement of the pulmonary artery with a lower iodine contrast concentration. However, iodine concentration has been found [9, 33] to have no effect on liver enhancement. The primary advantage of higher concentration of contrast medium is allowing a lower injection rate to provide the same amount of iodine injected for a specific time.

Finally, although the primary purpose of our study was to acquire scientific evidence and establish imaging protocol recommendations for CT of the chest in lung cancer, our results can be extrapolated to routine contrast-enhanced CT of the chest, abdomen, and pelvis for other neoplasms.

Our study had limitations. First, we focused on comparing a primary variable in the combined chest and abdominal CT scan protocol, which is the delay after the start of contrast administration. It can be argued that variation of other variables could overcome some of the problems detected in the evaluation of the images. However, the contrast injection parameters (overall contrast dose, delivery rate, injection duration, saline chaser volume and rate) and the scanning parameters (tube voltage and current, pitch, and others) were selected according to established clinical practices and existing evidence in the literature. Second, 110-kV tube voltage was used because of our existing manufacturer voltage configuration. When designing the study, we chose the 16-MDCT among the available scanners at our institution for being one of the most commonly used scanners at radiology facilities. Scanning times are similar for most 16-MDCT scanners, although that tube voltage is not so broadly extended. The lower tube voltage compared with 120 kV could increase attenuation values. Although further studies are necessary for confirmation, we routinely perform similar scanning protocols with other scanners using both 100 kV and 120 kV with similar clinically acceptable results. The same applies to tube current, which was fairly high in both protocols. Weight-based tube voltage and current should be applied in routine practice. Third, while reading the images, the observers could suspect which protocol was used in each case, leading to possible interpretation bias. To partially overcome this problem, the readers were asked to begin reading during the abdominal phase.

Conclusion

For patients with lung cancer, a single 60-second delayed acquisition for contrast-enhanced CT of the chest and abdomen is preferable to two separate acquisitions. It decreases contrast-related perivenous artifact, facilitates evaluation of mediastinal lymph node stations and pleural lesions, and improves tumor delineation. These benefits are achieved while the same abdominal enhancement and quality are maintained at lower but acceptable thoracic vascular enhancement and a lower radiation dose.

Acknowledgments

We thank Aaron Frodsham and Mariana Planells Alduvin for assistance in the linguistic revision process.

References

1. Ettinger DS, Wood D, Aisner DL, et al. NCCN Clinical Practice Guidelines in Oncology (NCCN Guidelines): non-small cell lung cancer, version 8.2017. www.nccn.org/professionals/physician_gls/pdf/nscl.pdf. July 14, 2017. Accessed August 8, 2017
2. Novello S, Barlesi F, Califano R, et al. Metastatic non-small-cell lung cancer: ESMO clinical practice guidelines for diagnosis, treatment and follow-up. *Ann Oncol* 2016; 27(suppl 5):v1–v27
3. Silvestri GA, Gonzalez AV, Jantz MA, et al. Methods for staging non-small cell lung cancer: diagnosis and management of lung cancer, 3rd ed—American College of Chest Physicians evidence-based clinical practice guidelines. *Chest* 2013; 143(5 suppl):e211S–e250S
4. National Institute for Health and Care Excellence website. Lung cancer: diagnosis and management—clinical guideline CG121. www.nice.org.uk/guidance/cg121. Published April 2011. Accessed June 1, 2017
5. Lim E, Baldwin D, Beckles M, et al. Guidelines on the radical management of patients with lung cancer. *Thorax* 2010; 65(suppl 3):1–27
6. Bae KT. Intravenous contrast medium administration and scan timing at CT: considerations and approaches. *Radiology* 2010; 256:32–61
7. Loubeyre P, Debard I, Nemoz C, Minh VA. Using thoracic helical CT to assess iodine concentration in a small volume of nonionic contrast medium during vascular opacification: a prospective study. *AJR* 2000; 174:783–787
8. Setty BN, Sahani DV, Ouellette-Piazzo K, Hahn PF, Shepard JA. Comparison of enhancement, image quality, cost, and adverse reactions using 2 different contrast medium concentrations for routine chest CT on 16-slice MDCT. *J Comput Assist Tomogr* 2006; 30:818–822
9. Behrendt FF, Mahnken AH, Stanzel S, et al. Intra-

individual comparison of contrast media concentrations for combined abdominal and thoracic MDCT. *AJR* 2008; 191:145–150

10. Mühlenbruch G, Behrendt FF, Eddahabi MA, et al. Which iodine concentration in chest CT? A prospective study in 300 patients. *Eur Radiol* 2008; 18:2826–2832
11. Behrendt FF, Plumhans C, Keil S, et al. Contrast enhancement in chest multidetector computed tomography: intraindividual comparison of 300 mg/ml versus 400 mg/ml iodinated contrast medium. *Acad Radiol* 2009; 16:144–149
12. Sigal-Cinqualbre AB, Hennequin R, Abada HT, Chen X, Paul JF. Low-kilovoltage multi-detector row chest CT in adults: feasibility and effect on image quality and iodine dose. *Radiology* 2004; 231:169–174
13. Mayer C, Meyer M, Fink C, et al. Potential for radiation dose savings in abdominal and chest CT using automatic tube voltage selection in combination with automatic tube current modulation. *AJR* 2014; 203:292–299
14. Lurz M, Lell MM, Wuest W, et al. Automated tube voltage selection in thoracoabdominal computed tomography at high pitch using a third-generation dual-source scanner: image quality and radiation dose performance. *Invest Radiol* 2015; 50:352–360
15. Hopper KD, Singapuri K, Finkel A. Body CT and oncologic imaging. *Radiology* 2000; 215:27–40
16. British Thoracic Society Standards of Care Committee. BTS statement on malignant mesothelioma in the UK, 2007. *Thorax* 2007; 62(suppl 2):1–19
17. Bae KT. Optimization of contrast enhancement in thoracic MDCT. *Radiol Clin North Am* 2010; 48:9–29
18. Williams S. General techniques for examinations discussing CT, biopsy and MRI. In: Nicholson T, ed. *Recommendations for cross-sectional imaging in cancer management*, 2nd ed. London, UK: Royal College of Radiologists, 2014
19. Fleischmann D, Kamaya A. Optimal vascular and parenchymal contrast enhancement: the current state of the art. *Radiol Clin North Am* 2009; 47:13–26
20. García Garrigós E, Arenas Jiménez JJ, Sánchez Payá J, Sirera Matilla M, Gayete Cara À. Computed tomography protocols used in staging bronchopulmonary carcinoma: results of a national survey. *Radiologia* 2016; 58:460–467
21. Szucs-Farkas Z, Strautz T, Patak MA, et al. Is body weight the most appropriate criterion to select patients eligible for low-dose pulmonary CT angiography? Analysis of objective and subjective image quality at 80 kVp in 100 patients. *Eur Radiol* 2009; 19:1914–1922
22. Hopper KD, Mosher TJ, Kasales CJ, TenHave TR, Tully DA, Weaver JS. Thoracic spiral CT: delivery of contrast material pushed with injectable saline solution in a power injector. *Radiology* 1997; 205:269–271
23. Haage P, Schmitz-Rode T, Hübner D, Piroth W, Günther RW. Reduction of contrast material dose and artifacts by a saline flush using a double power injector in helical CT of the thorax. *AJR* 2000; 174:1049–1053
24. Takao H, Nojo T, Ohtomo K. Use of a saline chaser in abdominal computed tomography: a systematic review. *Clin Imaging* 2009; 33:261–266
25. Sundaram B, Kuriakose JW, Stojanovska J, Watcharotone K, Parker RA, Kazerooni EA. Thoracic central venous evaluation: comparison of first-pass direct versus delayed-phase indirect multidetector CT venography. *Clin Imaging* 2015; 39:412–416
26. Wittram C. How I do it: CT pulmonary angiography. *AJR* 2007; 188:1255–1261
27. Shinagare AB, Okajima Y, Oxnard GR, et al. Unsuspected pulmonary embolism in lung cancer patients: comparison of clinical characteristics and outcome with suspected pulmonary embolism. *Lung Cancer* 2012; 78:161–166
28. Tsim S, Stobo DB, Alexander L, Kelly C, Blyth KG. The diagnostic performance of routinely acquired and reported computed tomography imaging in patients presenting with suspected pleural malignancy. *Lung Cancer* 2017; 103:38–43
29. Raj V, Kirke R, Bankart MJ, Entwisle J. Multidetector CT imaging of pleura: comparison of two contrast infusion protocols. *Br J Radiol* 2011; 84:796–799
30. Awai K, Kanematsu M, Kim T, et al. The optimal body size index with which to determine iodine dose for hepatic dynamic CT: a prospective multicenter study. *Radiology* 2016; 278:773–781
31. Yamashita Y, Komohara Y, Takahashi M, et al. Abdominal helical CT: evaluation of optimal doses of intravenous contrast material—a prospective randomized study. *Radiology* 2000; 216:718–723
32. Johnson PT, Fishman EK. IV contrast selection for MDCT: current thoughts and practice. *AJR* 2006; 186:406–415
33. Rengo M, Caruso D, De Cecco CN, et al. High concentration (400 mgI/mL) versus low concentration (320 mgI/mL) iodinated contrast media in multi detector computed tomography of the liver: a randomized, single centre, non-inferiority study. *Eur J Radiol* 2012; 81:3096–3101

FOR YOUR INFORMATION

A data supplement for this article can be viewed in the online version of the article at: www.ajronline.org.